





# Implementation of higher order sliding mode control of DC–DC buck converter fed permanent magnet DC motor with improved performance

Dhanasekar Ravikumar <sup>a,b</sup> and Ganesh Kumar Srinivasan <sup>b</sup>

<sup>a</sup>Department of Electrical and Electronics Engineering, Sri Sairam Institute of Technology, Chennai, Tamil Nadu, India; <sup>b</sup>Department of Electrical and Electronics Engineering, Anna University, Chennai, Tamil Nadu, India

## ABSTRACT

In this paper, an attempt is made to improve the performance of permanent magnet DC (PMDC) motor using third order sliding mode control. From the derived mathematical modelling for buck converter fed permanent magnet DC motor, expressions for both classical sliding surface (CSS) and proportional integral derivative sliding surface (PIDSS) with the third order sliding mode control is derived and compared analytically. Simulation work is done for PI controller, sliding mode control (SMC), third order CSS and third order PIDSS by using Matlab/Simulink to validate the performance of the above said controllers under no-load condition and various load torque conditions such as: constant load torque, frictional load torque, fan type load torque, propeller type load torque and undefined load torque. Experimental results are obtained with PMDC motor to validate the proposed control method for various speeds with different constant load torque conditions. Comparisons are carried out both in simulation and real time for PI controller, SMC, CSS and PIDSS based on the speed settling time and steady state error. Satisfactory results are obtained and presented in this paper.

## ARTICLE HISTORY

Received 1 October 2021  
Accepted 26 August 2022

## KEYWORDS

Buck converter; higher order sliding mode control; motor speed; PMDC motor

## 1. Introduction

DC motors are extensively applied in an industrial control application because of its robustness and broad range of speed-torque characteristics [1,2]. These applications require high exactness with broad range of speed control under disturbances. Permanent magnet direct current (PMDC) motor works with less friction and good acceleration/deceleration. The thermic characteristics of PMDC motor are decent when combined and thus it is applied in industrial applications with well behavioural controllers [3]. Recently, DC motors are involved for an energy management system. A bi-directional power packet router is expanded to drive the DC motor and the control of regenerative power in energy management systems [4]. DC motors are used in cart-pendulum systems which will move along the desired reference trajectories under external disturbances [5]. Limited angle rotary torque PMDC motor is designed and distinguished by limited operating range of torque with defined current [6]. DC motors are subjected to use with P, PI and PID controllers with firmware-based pulse width modulation and implemented in field programmable gate array based – controller to obtain the optimum performance [7]. Permanent magnet motor is designed to operate with mixed dc and ac signal and it is proposed in [8]. The motor vibration, noise and efficiency can be studied with various power frequencies ranging from

50 Hz to 3000 Hz [8]. Recent advancements in magnetic materials and their low cost makes PMDC motor more attractive for wheelchair drive applications [9]. The motion control of PMDC motor is adopted with reconfigurable micro architecture using IOT [10]. In [11], steady state current signal of DC motor is analyzed and identified with the inaccurate counting in the sensorless estimation of speed. Sensorless technique is adopted due to its robustness and cost effective.

Variable structure control (VSC) is a viable control which controls any kind of non-linear systems in an effective way. This increases the attraction of control engineers to implement the same for various practical applications [12]. VSC with SMC is especially meant for attracting to control the nonlinear systems due to its capabilities in invariance, robustness, order reduction and chattering free [13]. SMC is a variable structure approach which can be applicable to various types of non-linear systems. This approach involves discontinuous control law which forces the system trajectory into the specified sliding surface and maintains the trajectory in the surface. SMC is characterized by its new concept, robustness to uncertainties and low sensitive to parameter variations. Regardless of the robustness properties the major drawback is a chattering effect in real time implementation [14].

A complete survey of literary works associated with SMC is elaborated in Table 1.

**CONTACT** Dhanasekar Ravikumar [dhanasekar.eee@sairamit.edu.in](mailto:dhanasekar.eee@sairamit.edu.in) Department of Electrical and Electronics Engineering, Sri Sairam Institute of Technology, Chennai, Tamil Nadu, India, Department of Electrical and Electronics Engineering, Anna University, Chennai, Tamil Nadu, India

**Table 1.** Survey of previous research works in sliding mode.

Ref. No.	Year	Topology	Type of sliding mode	Features
[15]	2021	Buck converter	Finite time disturbance observer based sliding mode	Regulated angular speed of the DC motor under disturbances
[16]	2021	Buck converter	Adaptive Backstepping based Sliding Mode	Achieved speed control of DC motor
[17]	2021	Buck converter	Reduced order extended state observer-based event triggered sliding mode	Achieves better tracking performance better under load resistance disturbance and input voltage variation
[18]	2021	Synchronous buck converter	Digital current limited sliding mode	Achieved high dynamic performance
[19]	2020	Buck converter	Continuous dynamic sliding mode	Speed tracking of the DC motor under disturbances
[20]	2020	Buck converter	Sliding mode control strategy with maximized existence region	Excellent response in the output voltage without overshoot and undershoot
[21]	2020	Buck converter	Sliding mode control in combination with PI controller	Output voltage is controlled under changes in load resistance and input voltage
[22]	2020	Buck converter	Discretized quasi-sliding mode	Stabilizing the bus voltage in dc microgrids with constant power loads
[23]	2020	Buck converter	Discretized sliding mode	Eliminates steady state error and reduce the chattering phenomenon under uncertainties and load variations
[24]	2020	Buck converter	Discrete time fast terminal sliding mode	Obtained output voltage regulation with good transient response
[25]	2019	Three phase inverter	Cascade second order sliding mode	Accurate speed tracking of permanent magnet synchronous motor under disturbances
[26]	2019	Buck converter	Disturbance observer-based sliding mode	Angular velocity of the motor shaft is regulated under unmodeled load torque disturbance
[27]	2019	Servo system	Fractional order sliding mode	Speed tracking in the presence of external load disturbance
[28]	2018	Buck converter	Third order sliding mode	Speed tracking of the DC motor without load variations
[29]	2012	Buck converter	PID sliding mode	Speed tracking of the DC motor without load variations
[30]	2004	Buck converter	Sigma-Delta sliding mode	Regulation of speed under load disturbances

Terminal sliding mode controller with barrier function is non-linear dynamic systems which is presented to foregather the errors to zero in finite time. The results are compared with adaptive controller and the error tracking is better for terminal sliding mode controller than adaptive controller [31]. SMC plays an essential role in wind energy conversion systems. PID type terminal sliding mode control is rendered in the machine side converter and grid side converter. The controllers decrease the response time of the converters and it also improves the robustness under external disturbances [32]. PID type non-singular fast terminal sliding mode controller is proposed for industrial robotic manipulator. The stability of the controller is proven by Lyapunov theory. From the results, it is found that the controller reduces the steady state error and cancels the chattering [33]. Though first order SMC is simple, it introduces high frequency oscillations which degrade the performance of whole system. Higher order sliding mode control (HOSMC) is introduced to alleviate these oscillations. It gives better accuracy and reduces the chattering [34]. The chattering effect is eliminated by the using HOSM control approach. The HOSMC requires the awareness of time derivatives of the variables [35,36].

In [26], SMC is applied to the converter fed DC motor for constant load torque. Simulation work is presented to regulate the speed of the DC motor under constant load torque. Further, chattering is not eliminated under the presence of disturbance in the work. In [27], fractional order sliding mode controller is adopted for DC motor for constant load torque. In [28], only

the speed control of PMDC motor is achieved through higher order SMC in simulation without the investigation with load torque. But in this paper, higher order CSS and PIDSS are designed and implemented in tracking the speed of DC motor through buck converter.

### 1.1. Contributions

The significant contributions of this paper are listed as follows:

- Procedures for the implementation of third order classical sliding surface (CSS) and Proportional Integral Derivative Sliding Surface (PIDSS) for PMDC motor are completed.
- Servo and regulatory responses are obtained using PI controller, SMC, third order SMC with CSS and PIDSS for buck converter fed DC motor via simulation study and experimental setup. Further, performance of the above said controllers are compared and presented.
- The suggested control law avoids overshoot, rejects disturbance, maintains sufficient control quality in the larger working range, and is more resilient to uncertainties.

### 1.2. Paper organization

This paper describes the design procedure of third order PIDSS and third order CSS for buck converter fed PMDC motor. Section 2 explains the modelling of

buck converter fed PMDC motor, section 3 explains the generalized procedure for designing the control law, section 4 discussed about the design of CSS (third order), section 5 discussed about the third order PIDSS, section 6 discussed the simulation results, section 7 discussed about experimental setup and results obtained. Finally, conclusion is drafted in section 8.

## 2. Modelling of buck converter fed PMDC motor

Figure 1 shows the implementation of servo and regulatory responses of buck converter fed PMDC motor via PI controller, SMC and third order SMC with CSS and PIDSS. Further, it is intended to compare the performance of above said controllers under no-load and loaded conditions.

The mathematical model of the combination of buck converter with PMDC motor for the proposed control can be given as:

$$\begin{aligned}\frac{d\omega}{dt} &= -Z_3\omega + Z_1i_a - Z_8T_L \\ \frac{di_a}{dt} &= -Z_6\omega - Z_2i_a + Z_5v_a \\ \frac{dv_a}{dt} &= -Z_4i_a + Z_4i_L \\ \frac{di_L}{dt} &= -Z_7v_a + Z_7Eu\end{aligned}\quad (1)$$

where  $Z_1 = \frac{K_t}{J}$ ;  $Z_2 = \frac{R_a}{L_a}$ ;  $Z_3 = \frac{B}{J}$ ;  $Z_4 = \frac{1}{C}$ ;  $Z_5 = \frac{1}{L_a}$ ;  $Z_6 = \frac{K_e}{L_a}$ ;  $Z_7 = \frac{1}{L}$ ;  $Z_8 = \frac{1}{J}$ .

The PMDC motor and buck converter parameters are given as:

$\omega$	Motor speed in rad/sec
$L$	Inductance in Henry
$C$	Capacitance in Farad

$i_a$	Armature current in Ampere
$T_L$	Load torque in Nm
$J$	Moment of inertia in $\text{kgm}^2$
$v_a$	Armature voltage in Volts
$E$	Input voltage to the buck converter in Volts
$i_L$	Inductor current in Ampere
$K_t$	Torque constant in Nm/A
$K_e$	Backemf constant in V/rpm
$R_a$	Armature resistance in Ohm
$L_a$	Armature inductance in Henry
$u$	Control input
$S$	IGBT Switch
$D$	Diode

## 3. Generalized procedure for designing the control law for HOSMC

The generalized procedure for designing the control law for HOSMC is explained as below:

**Step 1:** Consider a sliding surface  $S = (\frac{d}{dt} + \lambda)^{n-1}$  for the system

$\dot{X} = A(X, t) + B(X, t)u$  in which the control input "u" drive the system to the desired response. (where "n" is the order of the system and "λ" is the positive constant).

**Step 2:** Compute the derivatives of sliding surface,  $S, \dot{S}, \ddot{S}$ .

**Step 3:** Derive the equivalent (continuous) signal ' $u_{eq}$ ' through the derivative of sliding surface by computing  $S, \dot{S}, \ddot{S} = 0$ .

**Step 4:** Design the switching signal ' $u_{sw}$ ' using Homogeneity approach [37] which results in faster convergence to bring the system into the desired response.

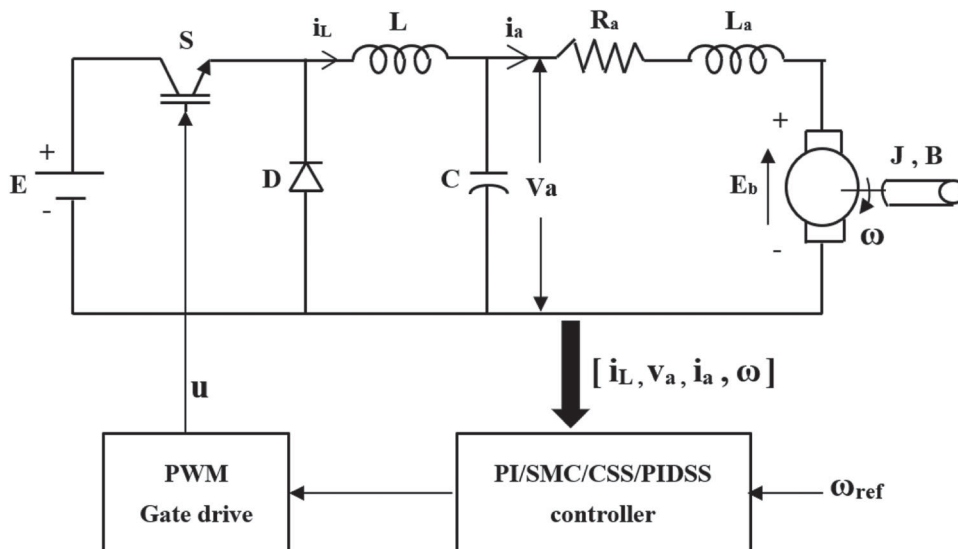


**Figure 1.** Controller development and implementation for buck converter driven PMDC motor.

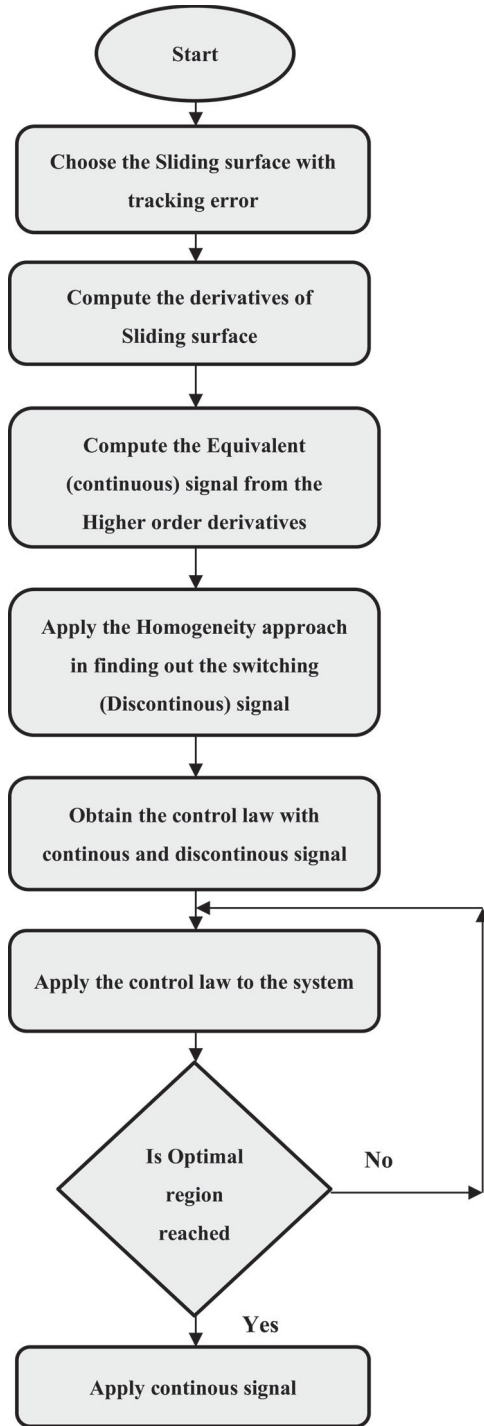


**Figure 2.** Flowchart for CSS algorithm.

**Step 5:** Formulate the final control law  $u = u_{eq} + u_{sw}$  which consists of two additive signals; continuous signal  $'u_{eq}'$  and discontinuous signal  $'u_{sw}'$ .

The above-mentioned algorithm is summarized as flowchart and it is shown in Figure 2.

#### 4. Design of third order CSS for buck converter fed PMDC motor

The classical sliding surface (CSS)  $'\delta'$  is given as in Equation (2)

$$\delta = Ce + \frac{de}{dt} \quad (2)$$

Let "e" is taken as the speed error which is the difference between reference speed " $\omega_{ref}$ " and the actual speed " $\omega$ ".

where  $C > 0$  is positive real value.

$$\delta = C(\omega_{ref} - \omega) - \dot{\omega} \quad (3)$$

$$\delta = C(\omega_{ref} - \omega) + Z_3\omega - Z_1i_a + Z_8T_L \quad (4)$$

According to the Equation (4), the speed error decays to zero when the sliding surface reaches zero.

The first derivative of the classical sliding surface  $'\delta'$  is given as in Equation (5),

$$\dot{\delta} = ((\omega A_1) + (i_a A_2) - (Z_1 Z_5 v_a) + (T_L A_3)) \quad (5)$$

where,

$$A_1 = ((CZ_3) - (Z_3^2) + (Z_1 Z_6))$$

$$A_2 = ((Z_3 Z_1) - (CZ_1) + (Z_1 Z_2))$$

$$A_3 = ((CZ_8) - (Z_3 Z_8))$$

The second derivative of the classical sliding surface  $'\delta'$  is given as in Equation (6),

$$\ddot{\delta} = ((\omega A_4) + (i_a A_5) + (v_a A_6) - (Z_1 Z_5 Z_4 i_L) + (T_L A_7)) \quad (6)$$

where,

$$A_4 = ((Z_3^3) - (CZ_3^2) - (Z_1 Z_6 Z_3) - (Z_1 Z_6 Z_3) + (CZ_1 Z_6) - (Z_1 Z_6 Z_2))$$

$$A_5 = ((CZ_1 Z_3) - (Z_1 Z_3^2) + (Z_1^2 Z_6) - (Z_2 Z_3 Z_1) + (CZ_2 Z_1) - (Z_1 Z_2^2) + (Z_1 Z_5 Z_4))$$

$$A_6 = ((Z_1 Z_5 Z_3) - (CZ_1 Z_5) + (Z_1 Z_5 Z_2))$$

$$A_7 = ((Z_8 Z_3^2) - (CZ_3 Z_8) - (Z_1 Z_8 Z_6))$$

The third derivative of the classical sliding surface  $'\delta'$  is given as in Equation (7), which is the combination of motor speed, armature current, armature voltage and inductor current.

$$\ddot{\delta} = \omega(-Z_3 A_8 - Z_6 A_9) + i_a(Z_1 A_8 - Z_2 A_9 - Z_4 A_{10}) + v_a(Z_5 A_9 - Z_7 A_{11}) + Z_4 A_{10} i_L - A_8 Z_8 T_L + Z_7 A_{11} E u \quad (7)$$

where,

$$A_8 = Z_3^3 - CZ_3^2 - Z_1 Z_6 Z_3 - Z_1 Z_6 Z_3 + CZ_1 Z_6 - Z_1 Z_6 Z_2$$

$$A_9 = CZ_1Z_3 - Z_1Z_3^2 + Z_1^2Z_6 - Z_2Z_1Z_3 + Z_2CZ_1 \\ - Z_1Z_2^2 + Z_5Z_1Z_4$$

$$A_{10} = Z_5Z_1Z_3 - CZ_1Z_5 + Z_1Z_5Z_2$$

$$A_{11} = -Z_1Z_5Z_4$$

The finite time convergence is achieved by using homogeneity approach [37].

Take

$$\ddot{\delta} = K \quad (8)$$

where  $K = -\alpha \text{sgn} \left( \ddot{\delta} + \beta_2 (|\delta|^2 + |\dot{\delta}|^3)^{\frac{1}{6}} \text{sgn}(|\dot{\delta}|) \right) + \beta_1 |\delta|^{\frac{2}{3}} \text{sgn}(\delta)$ .

The values of  $\alpha$ ,  $\beta_1$  and  $\beta_2$  are taken as positive constants. In third order CSS, the sliding coefficient “C” is chosen as 15 by trial and error method [38] such that the speed tracking profile is good without disturbances. The control parameters  $\alpha$ ,  $\beta_1$  and  $\beta_2$  are chosen as  $25 \times 10^{100}$ , 312 and 18,000, so that the control law remains positive and bounded within 1. Equation (7) is written as,

$$K = \omega(-Z_3A_8 - Z_6A_9) + i_a(Z_1A_8 - Z_2A_9 - Z_4A_{10}) \\ + V_a(Z_5A_9 - Z_7A_{11}) + Z_4A_{10}i_L \\ - A_8Z_8T_L + Z_7A_{11}Eu \quad (9)$$

Equation (9) is given as,

$$K = f + Mu \quad (10)$$

where,

$$f = \omega(-A_3Z_8 - A_6Z_9) + i_a(A_1Z_8 - A_2Z_9 - A_4Z_{10}) \\ + V_a(A_5Z_9 - A_7Z_{11}) + A_4Z_{10}i_L - A_8Z_8T_L$$

$$M = A_7Z_{11}E$$

From the Equation (10), the control input is given as the combination of switching signal “ $u_{sw}$ ” and the continuous signal “ $u_{eq}$ ”.

$$u = \frac{K - f}{M} \quad (11)$$

where  $u_{sw} = \frac{K}{M}$  and  $u_{eq} = \frac{f}{M}$

Initially the supply voltage to the converter is given as 15 V. The reference speed of the motor is set as 50% of the rated speed (i.e.) 750 rpm with zero load torque condition.

## 5. Design of third order PIDSS for buck converter fed PMDC motor

In this section, sliding surface of speed error ( $e$ ) is written with proportional, integral and derivative values for

regulating the speed of the PMDC motor under various load torque conditions.

$$e = \omega_{ref} - \omega \quad (12)$$

where ‘ $\omega_{ref}$ ’ is the reference speed and ‘ $\omega$ ’ is the actual speed.

Now the Proportional, Integral and Derivative Sliding surface (PIDSS) is chosen as

$$\varphi = D_1e + D_2 \int e dt + D_3 \frac{de}{dt} \quad (13)$$

where  $D_1$ ,  $D_2$  and  $D_3$  are the proportional, integral and derivative gains

$$\varphi = D_1(\omega_{ref} - \omega) + D_2 \int (\omega_{ref} - \omega) dt \\ - D_3(-Z_3\omega + Z_1i_a - Z_8T_L) \quad (14)$$

The first derivative of ‘ $\varphi$ ’ is given as in Equation (15).

$$\dot{\varphi} = \omega(D_1Z_3 - D_2 - D_3Z_3^2 + D_3Z_1Z_6) \\ + i_a(-D_1Z_1 + D_3Z_3Z_1 + D_3Z_2Z_1) \\ + v_a(-D_3Z_1Z_5) + D_2\omega_{ref} \\ + Z_8T_L(D_1 - D_3Z_3) \quad (15)$$

The second derivative of ‘ $\varphi$ ’ is given as in Equation (16).

$$\ddot{\varphi} = \omega(-Z_3A_1 - A_2Z_6) + i_a(Z_1A_1 - Z_2A_2 - Z_4A_3) \\ + v_aZ_5A_2 + Z_4A_3i_L + Z_8T_LA_1 \quad (16)$$

where,

$$A_1 = (D_1Z_3 - D_2 - D_3Z_3^2 + D_3Z_1Z_6)$$

$$A_2 = (-D_1Z_1 + D_3Z_3Z_1 + D_3Z_2Z_1)$$

$$A_3 = (-D_3Z_5Z_1)$$

$$A_4 = (-Z_3A_1 - Z_6A_2)$$

$$A_5 = (Z_1A_1 - Z_2A_2 - Z_4A_3)$$

The third derivative of  $\varphi$  is given as in Equation (17), which is the combination of actual speed, armature current, armature voltage, inductor current and load torque.

$$\ddot{\delta} = \omega(-Z_3A_4 - A_5Z_6) + i_a(Z_1A_4 - Z_2A_5 - Z_5A_2Z_4) \\ + v_a(Z_5A_5 - Z_4A_3Z_7) + Z_5A_2Z_4i_L + Z_4A_3Z_7Eu \\ - Z_8T_LA_4 \quad (17)$$

Taking  $\ddot{\delta} = H$ , which is a Homogeneity approach.

where,  $H = -\alpha \text{sgn} \left( \ddot{\delta} + \beta_2 (|\delta|^2 + |\dot{\delta}|^3)^{\frac{1}{6}} \text{sgn}(|\dot{\delta}|) + \beta_1 |\delta|^{\frac{2}{3}} \text{sgn}(\delta) \right)$

By Ziegler-Nicholos (ZN) [39] approach, the values of  $D_1, D_2$  and  $D_3$  are chosen as 15, 0.15 and 0.3, respectively. The values of  $\alpha, \beta_1, \beta_2$  are taken as positive constants and it is chosen carefully to reach the sliding surface to zero. The control parameters are chosen  $\alpha, \beta_1, \beta_2$  as  $18 \times 10^{100}, 139$  and  $18,000$ , so that the control law remains positive and the control signal “u” value switch between “0” and “1”.

$$H = \rho + \sigma u \quad (18)$$

where

$$\rho = \omega(-Z_3 A_4 - A_5 Z_6) + i_a(Z_1 A_4 - Z_2 A_5 - Z_5 A_2 Z_4) + v_a(Z_5 A_5 - Z_4 A_3 Z_7) + Z_5 A_2 Z_4 i_L - Z_8 T_L A_4$$

$$\sigma = Z_4 A_3 Z_7 E$$

The control input is given in Equation (19),

$$u = \frac{H - \rho}{\sigma} \quad (19)$$

## 6. Simulation results and discussions

It is planned to test the performance of PI controller, SMC, CSS and PIDSS with the proposed system. The proposed HOSMC is validated through the Matlab simulation for no-load condition and different load torque conditions with the specifications as mentioned in Table 2. Any system's performance can be increased with the correct controller tuning. The Ziegler-Nicholos (ZN) [39] approach is utilized for the PI controller to determine the values of proportional constant “Kp” and integral constant “Ki”. The gain values of Kp and Ki is denoted as 8 and 0.067 respectively.

The traditional method of implementing SMC is directly based on the governing law. In various applications the control input will be either positive or negative

**Table 2.** Specifications for the proposed work.

PMDC Motor		Buck Converter	
$P_o$ : Power	18 W	$L$ : Inductance	1.06 mH
$V_a$ : Voltage	12 V	$C$ : Capacitance	1000 $\mu$ F
$I_a$ : Current	1.5 A	$E$ : Input Voltage	15 V
$T$ : Torque	1 kG cm	$F$ : Frequency	5 kHz
$R_a$ : Armature resistance	2.6 $\Omega$	$S$ : Switch	IGBT
$L_a$ : Armature inductance	712.85 mH	$D$	Diode
$K_e$ : Backemf constant	0.05022 V s/rad	<i>Feedback variables</i>	
$J$ : Moment of Inertia	8.86138e-5 kgm <sup>2</sup>	PI controller	$\omega$
$B$ : Viscous friction coefficient	9.6894e-5 N-m/rad	SMC	$i_L, v_a$
$K_t$ : Torque constant	0.05022 N-m/A	CSS	$i_L, i_a, v_a, \omega$
$\omega$ : Speed	157 rad/s	PIDSS	$i_L, i_a, v_a, \omega$

decision. So in SMC, the control input is given as,

$$u = \frac{1}{2}(1 - \text{sgn}(S)) \quad (20)$$

where  $S$  is the sliding surface. Sliding surface is chosen as the error input, which is the difference between reference and actual speed. When this control law is applied directly, it causes systems to turn on and off at very high frequencies, which causes unwanted chattering in the system. In Higher order CSS, third order sliding surface is chosen to eliminate the chattering and also for smooth control of PMDC motor.

Feedback variables used for the closed loop operation of PI controller, SMC, CSS and PIDSS are mentioned in Table 2.

The performance of PI, SMC, CSS and PIDSS are tested when the load torque value is zero, constant, proportional to speed, proportional to square of speed, proportional to cube of speed and undefined values.

### 6.1. Under no load condition

The simulation is gone through MATLAB/Simulink under no-load condition (Load torque  $T_L = 0$  N-m) to show the effectiveness of PIDSS. The reference speed profile is shown in the Figure 3. Initially, the motor is rotating at the angular speed of  $\omega = 39.25$  rad/sec, i.e. 0.25 p.u. from the time period of 0 s to 4 s, then the speed climbs up to  $\omega = 78.5$  rad/sec, i.e. 0.5 p.u. from 4 s to 7 s, then the speed increased to  $\omega = 117.75$  rad/sec, i.e. 0.75 p.u. from the time duration of 7 s to 10 s and finally the speed reaches to the rated speed of  $\omega = 157$  rad/sec, i.e. 1 p.u. from 10 s to 11 s.

Figure 4 shows the changes in armature current for the reference speed profile shown in Figure 3. Figure 5 shows the integral square error of PI controller, SMC, CSS and PIDSS. The integral square error of PIDSS is minimum in comparison with PI controller, SMC and CSS. Figure 6 shows the sliding surface evolutions of CSS and PIDSS evolutions under no-load conditions. Figure 7 shows the speed response comparison between

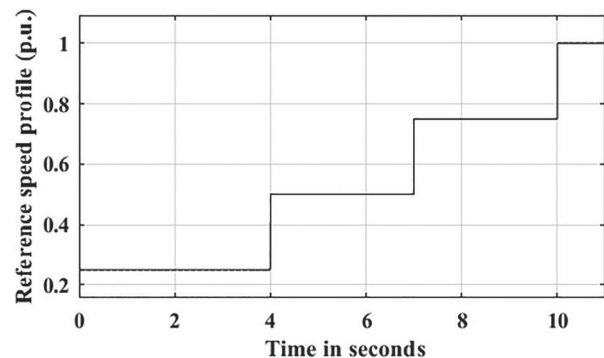


**Figure 3.** Reference speed.

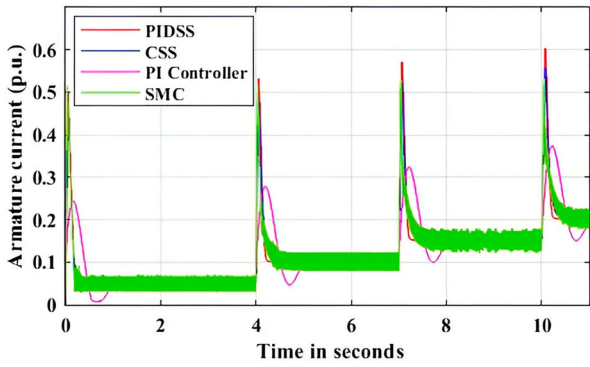


**Figure 4.** Comparison between PI controller, SMC, CSS and PIDSS (Armature current evolutions under no-load condition).

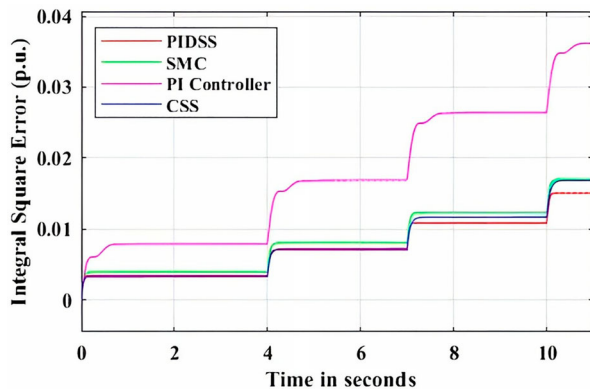


**Figure 5.** Integral square error under no-load conditions for various reference speeds.

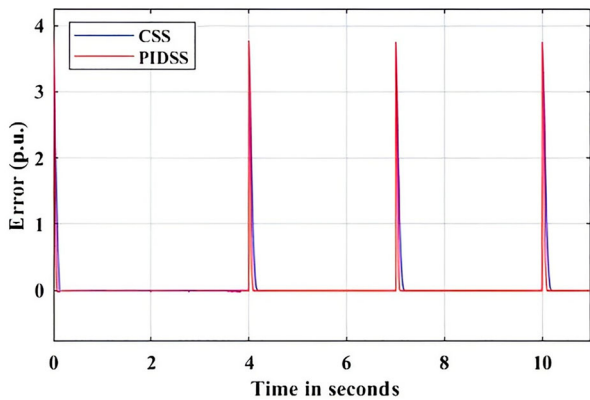


**Figure 6.** Comparison between CSS and PIDSS evolutions under no-load conditions.

PI controller, SMC, CSS and PIDSS under no-load conditions. However, after varying the speed under no-load conditions, it can be seen that the PIDSS performs better than the other control methodologies in terms of peak overshoot and recovery time.

### 6.2. Constant load torque

The robustness of the controllers towards constant load torque is verified under various speeds. The details of machine operation for the selected speed profile and load torque profile is listed in Table 3. The selected

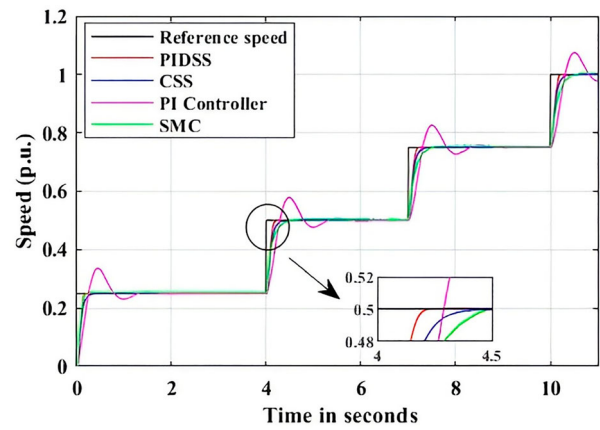


**Figure 7.** Speed response comparison between PI controller, SMC, CSS and PIDSS under no-load conditions.

**Table 3.** Details of machine operation.

Time in seconds	Reference speed profile (rad/sec)	Reference speed profile (p.u.)	Load torque profile (p.u.)
0–4 s	78.5	0.5	–
4–6 s	78.5	0.5	0.5
6–8 s	157	1	0.5
8–10 s	157	1	1
10–11 s	94.2	0.6	1

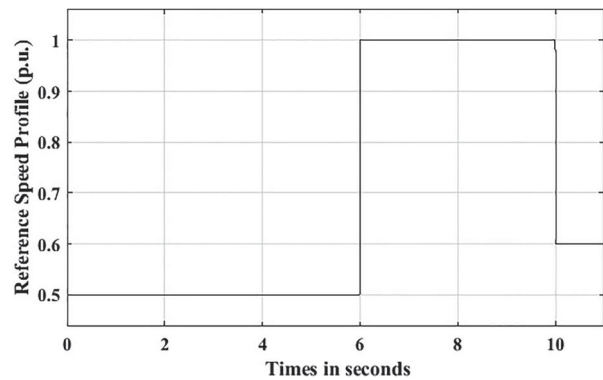


**Figure 8.** Reference speed.

speed profile and load torque profile is shown in Figures 8 and 9.

The simulation results for PI controller, SMC, CSS and PIDSS are compared for constant load torque. When the load torque changes at 4 and 8 s, the PIDSS has clear advantage over CSS in recovery time and disturbance suppression. The convergence of the sliding surface of PIDSS is soon compared with CSS. While starting, the armature current exhibits no peak overshoot beyond the rated load current which implies the soft starting of PMDC motor. The speed of PMDC motor is settled soon without chattering by PIDSS rather than PI, SMC and CSS for the load torque profile as shown in Figure 9.

For constant load torque condition with the reference values of speed and load torque as shown

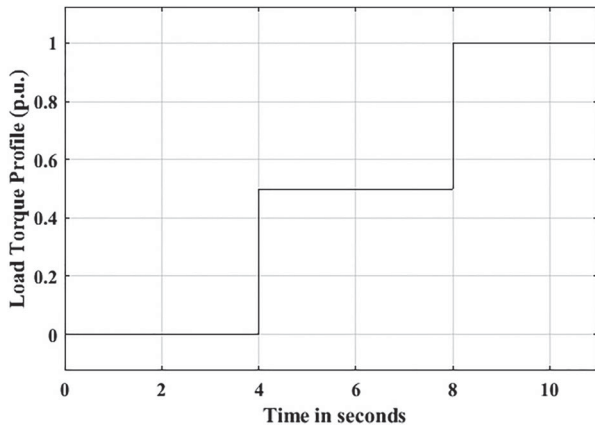


Figure 9. Load torque.

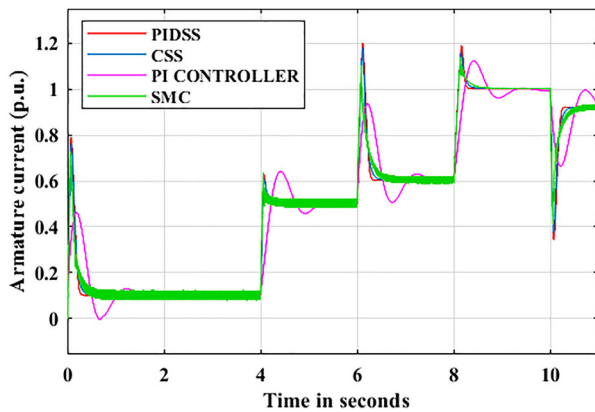


Figure 10. Comparison between PI controller, SMC, CSS and PIDSS (armature current evolutions for constant load torque).

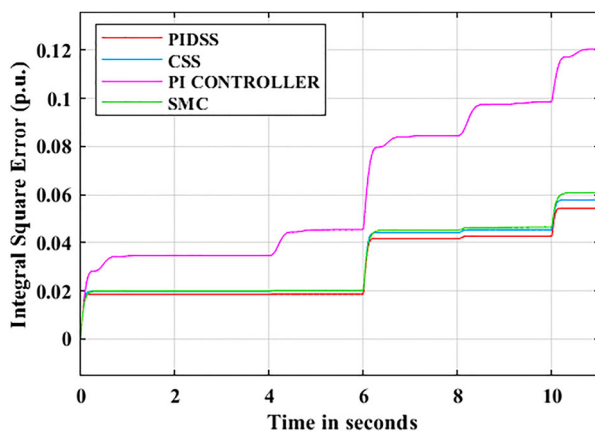


Figure 11. Integral square error for constant load torque.

in Table 3, simulation results for the comparison of armature current evolutions, Integral square error, sliding surface evolutions and speed are shown in Figures 10–13. Figure 13 depicts the settling time comparison for PI, SMC, CSS and PIDSS for constant load torque. From the above it is found that the performance of PIDSS is better than PI, SMC and CSS.

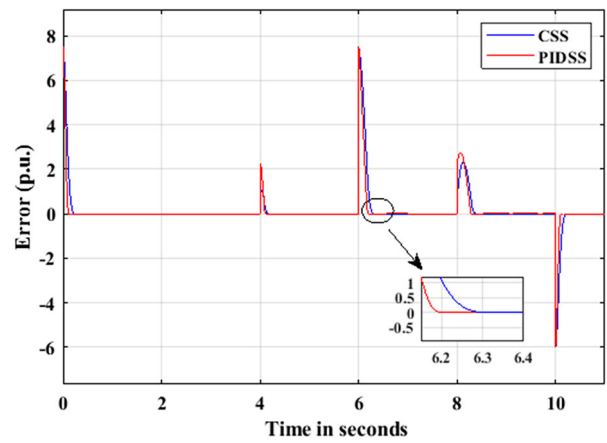


Figure 12. Comparison between CSS and PIDSS evolutions for constant load torque.

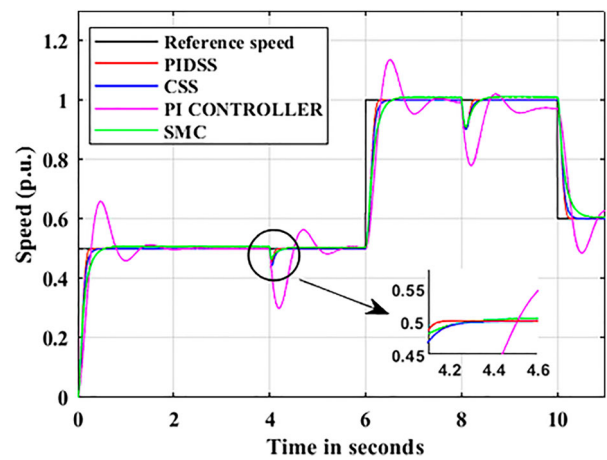


Figure 13. Speed response comparison between PI controller, SMC, CSS and PIDSS for constant load torque.

### 6.3. Frictional load torque

For frictional load, the load torque is directly proportional to speed ( $T_L = K_1\omega$ ). The proportionality constant  $K_1$  is chosen as  $3.8 \times 10^{-4}$ , so that the load torque remains within the limits. For the speed reference as shown in Figure 8, the load torque reference is calculated using  $T_L = K_1\omega$  and it shown in Figure 14. Figure 15 shows the sliding surface evolutions of CSS and PIDSS for frictional load torque. The settling time for the speed of the PMDC motor is less for PIDSS in comparison with CSS, SMC and PI algorithms and it is shown in Figure 16.

### 6.4. Fan type load torque

For fan load, the load torque is directly proportional to speed ( $T_L = K_2\omega^2$ ). The proportionality constant  $K_2$  is chosen as  $2.44 \times 10^{-6}$ . For the reference speed profile shown in Figure 8, fan type load torque is shown in Figure 17. Figure 18 shows the sliding surface evolutions of CSS and PIDSS for fan type load torque. The settling speed of the PMDC motor and speed tracking

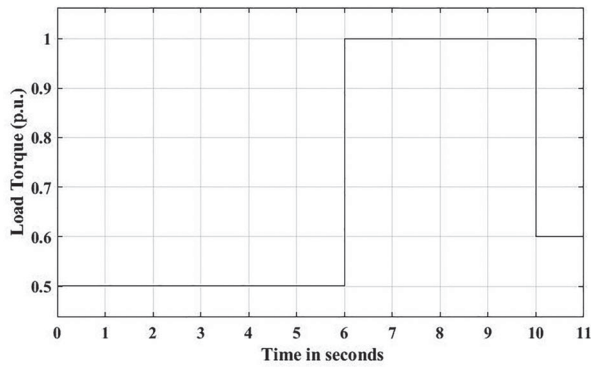


Figure 14. Load torque – ( $T_L \propto \omega$ ).

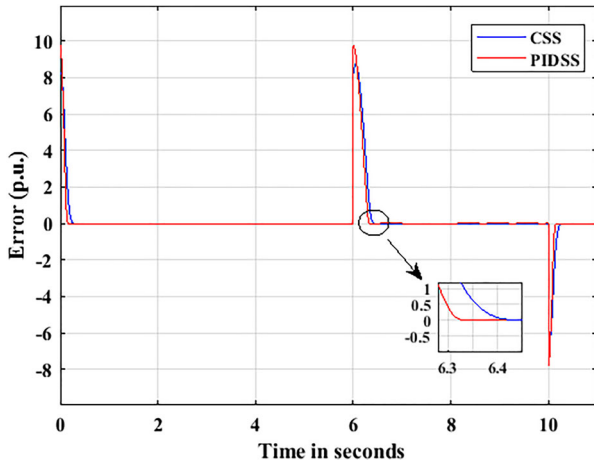


Figure 15. Comparison between CSS and PIDSS evolutions for frictional load torque.

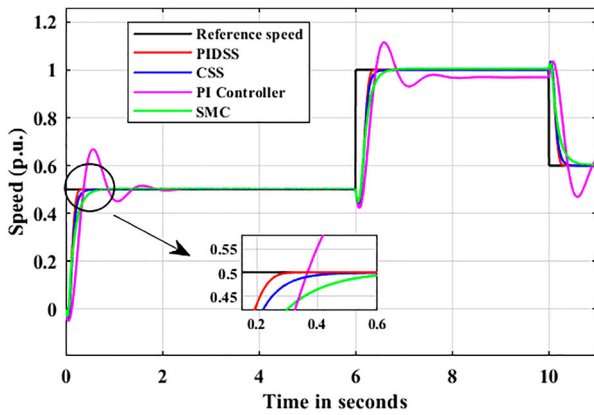


Figure 16. Speed response comparison between PI controller, SMC, CSS and PIDSS for frictional load torque.

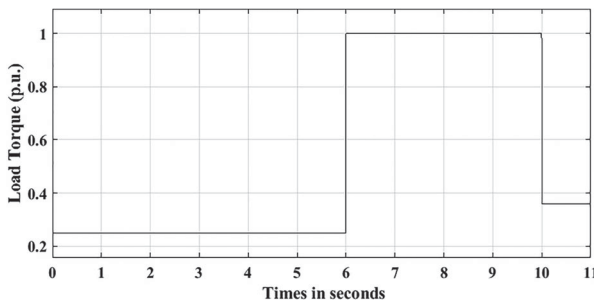


Figure 17. Load torque – ( $T_L \propto \omega^2$ ).

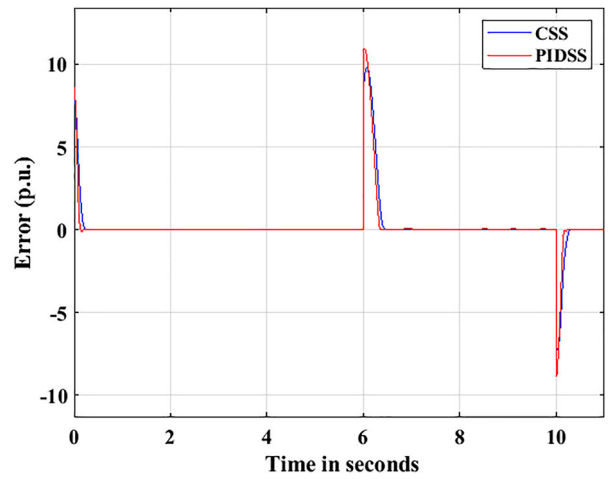


Figure 18. Comparison between CSS and PIDSS evolutions for fan type load torque.

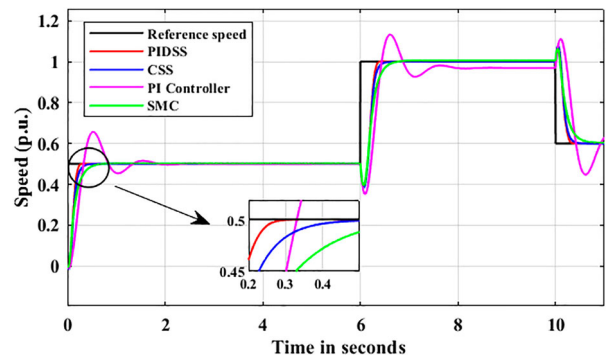


Figure 19. Speed response comparison between PI controller, SMC, CSS and PIDSS for fan type load torque.

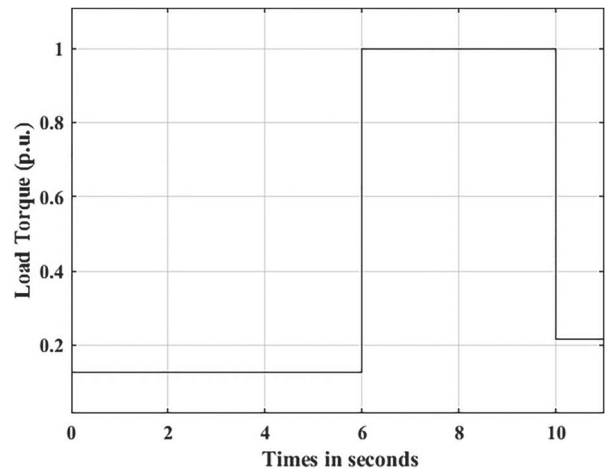
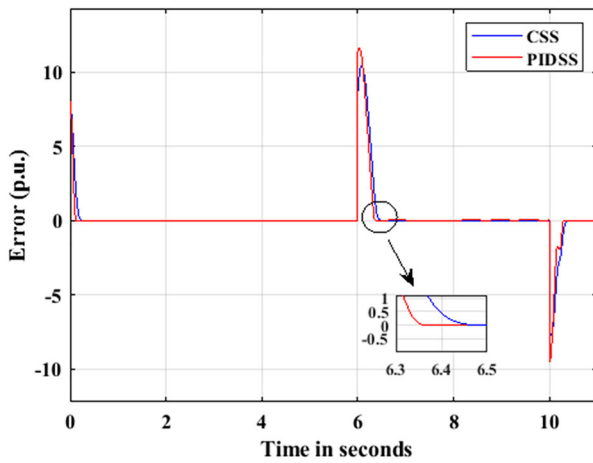


Figure 20. Load torque – ( $T_L \propto \omega^3$ ).

is better for PIDSS in comparison with CSS, SMC and PI algorithms and it is shown in Figure 19.

### 6.5. Propeller type load torque

For propeller load, the load torque is directly proportional to speed ( $T_L = K_3 \omega^3$ ). The proportionality constant  $K_3$  is chosen as  $1.55 \times 10^{-8}$ . For the reference speed profile shown in Figure 8, the load torque obtained is shown in Figure 20. Figure 21 shows the



**Figure 21.** Comparison between CSS and PIDSS sliding surface evolutions for propeller load torque.

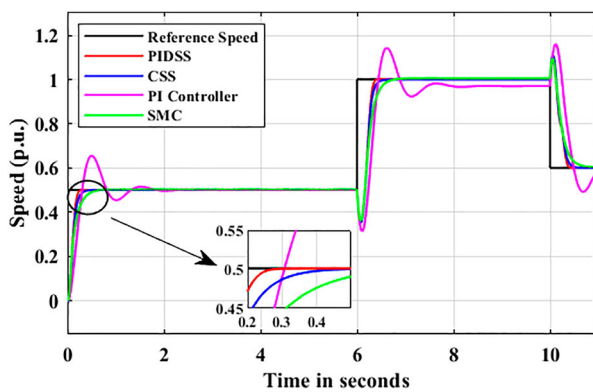


**Figure 22.** Speed response comparison between PI controller, SMC, CSS and PIDSS for propeller load torque.

sliding surface evolutions of CSS and PIDSS for propeller type load torque. Figure 22 shows the speed evolutions of PIDSS, CSS, SMC and PI controller.

From the above simulation study, it is found that PIDSS performs better than PI, SMC and CSS for no-load condition, constant load torque, frictional load torque, fan type load torque and propeller type load torque. Speed settling time comparison is shown in Table 4. From the comparison results it can be seen that the PIDSS settles soon compared with CSS, SMC and PI controller for constant load torque, frictional load torque, fan type load torque and propeller type load torque.

## 6.6. Undefined type load torque

In [15], a time varying sinusoidal waveform is chosen to show the performance of the algorithm, but in this paper, two undefined load torques (Figures 23 and 26) are selected to study the effectiveness of PIDSS. The undefined load torque-1 is shown in Figure 23 is applied on the motor for the reference speed profile as shown in Figure 8. The simulation result for the convergence of sliding surface and speed is shown in Figures 24 and 25 for the undefined load torque profile-1.

The comparison between PI controller, SMC, CSS and PIDSS for undefined load torque-1 is shown in Table 5. For the undefined load torque-1, the PIDSS settles the speed faster than CSS, SMC and PI controller.

The undefined load torque-2 is shown in Figure 26 and it is tested on the PMDC motor for the reference

**Table 4.** Comparison of PI, SMC, CSS and PIDSS.

Time in seconds	Reference speed in rad/sec	Reference speed in per unit	Load torque $T_L$ (p.u.)	Speed settling time in seconds				Steady state error %			
				PIDSS	CSS	SMC	PI	PIDSS	CSS	SMC	PI
<i>(a) Under no-load condition</i>											
0.0–4.0	39.25	0.25	0	0.226	0.384	0.865	1.810	–	–	–	–
4.0–7.0	78.5	0.5	0	0.227	0.392	0.887	1.921	–	0.02%	0.03%	0.03%
7.0–10.0	117.75	0.75	0	0.254	0.401	0.637	1.943	–	–	–	0.05%
10.0–11.0	157	1	0	0.491	0.635	0.737	0.987	–	–	–	0.02%
<i>(b) Constant load torque</i>											
0.0–4.0	78.5	0.5	0	0.226	0.384	0.865	1.810	–	–	–	–
4.0–6.0	78.5	0.5	0.5	0.142	0.289	0.435	1.913	–	–	–	–
6.0–8.0	157	1	0.5	0.258	0.405	0.825	1.948	–	–	–	–
8.0–10.0	157	1	1	0.247	0.395	0.628	–	–	–	–	3.8%
10.0–11.0	94.2	0.6	1	0.237	0.384	0.830	–	–	–	–	3.8%
<i>(c) Frictional load torque</i>											
0.0–6.0	78.5	0.5	0.5	0.279	0.458	0.736	2.111	–	–	–	–
6.0–10.0	157	1	1	0.342	0.489	0.774	–	–	–	–	4%
10.0–11.0	94.2	0.6	0.6	0.268	0.447	0.838	–	–	–	0.05%	4%
<i>(d) Fan type load torque</i>											
0.0–6.0	78.5	0.5	0.25	0.247	0.468	0.754	2.205	–	–	–	–
6.0–10.0	157	1	1	0.384	0.563	0.796	–	–	–	–	4%
10.0–11.0	94.2	0.6	0.36	0.310	0.458	0.866	–	–	–	0.04%	4%
<i>(e) Propeller load torque</i>											
0.0–6.0	78.5	0.5	0.125	0.268	0.532	0.785	2.322	–	–	–	–
6.0–10.0	157	1	1	0.426	0.605	0.930	–	–	–	0.045%	3.8%
10.0–11.0	94.2	0.6	0.216	0.405	0.584	0.931	–	–	–	–	3.8%

speed profile as shown in Figure 8. The CSS, PIDSS, SMC and PI controller performance is compared for the undefined load torque profile-2. The simulation result for the convergence of sliding surface and speed is shown in Figures 27 and 28.

For the undefined load torque-2, the comparative study is shown in Table 6. From the table, it is found that the PIDSS converges faster in comparison with CSS, SMC and PI controller for the reference speed of 0.5, 1 and 0.6 p.u.

From the above simulation study it can be concluded that, PIDSS settles faster than CSS, SMC and PI controller for the servo and regulatory operations of PMDC motor.

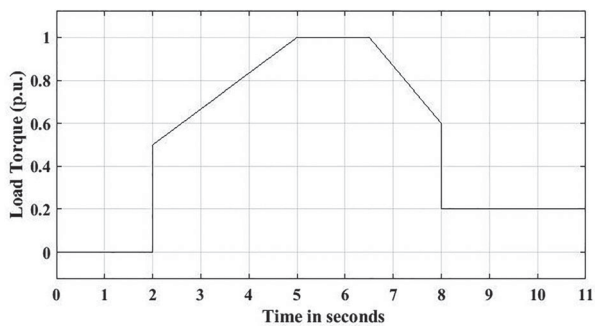


Figure 23. Undefined load torque-1.

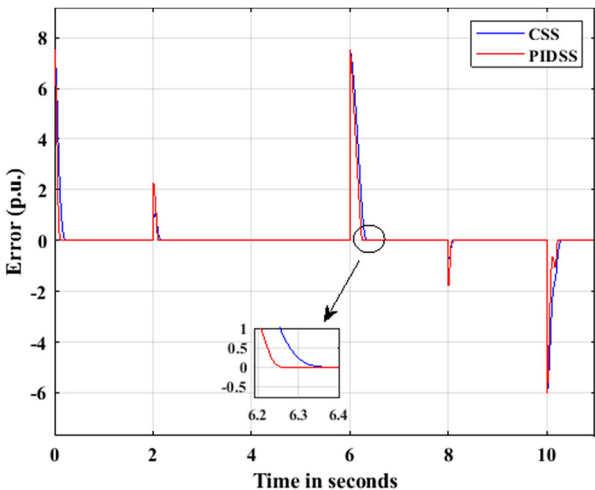


Figure 24. Comparison between CSS and PIDSS sliding surface evolutions for undefined load torque-1.

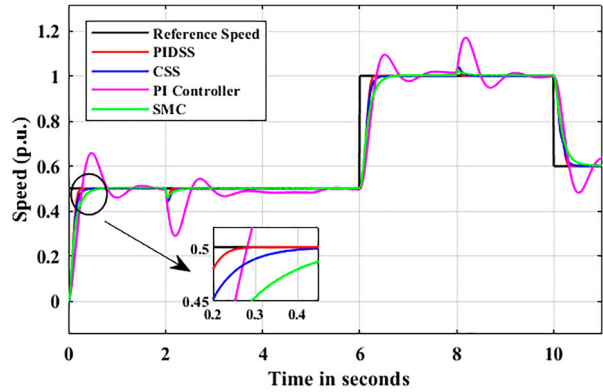


Figure 25. Speed response comparison between PI controller, SMC, CSS and PIDSS for undefined load torque-1.

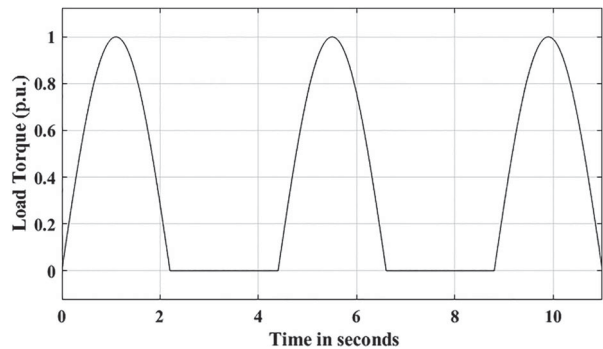


Figure 26. Undefined load torque-2.

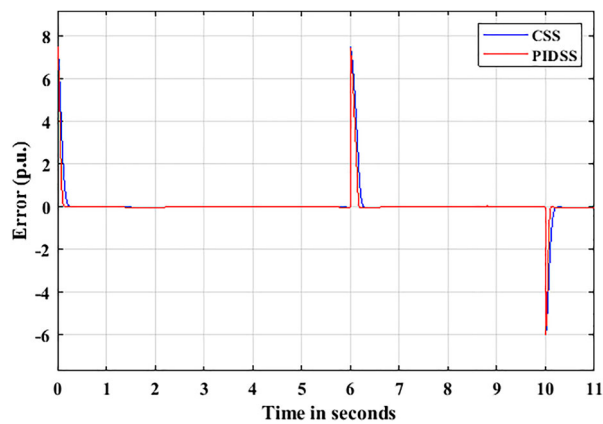


Figure 27. Comparison between CSS and PIDSS sliding surface evolutions for undefined load torque-2.

### 7. Experimental setup and discussions

In order to validate the simulation results, it is decided to test the performance of PIDSS using real time implementation. Further with the available of PMDC motor,

Table 5. Comparison of PI, SMC, CSS and PIDSS for undefined load torque-1.

Time in seconds	Reference speed in rad/sec	Load torque $T_L$ (p.u.) and reference speed (p.u.) variations	Speed settling time in seconds			
			PIDSS	CSS	SMC	PI
0.0–6.0	78.5	(i) 0 p.u load torque from 0 to 2 s for the reference speed 0.5 p.u.	0.236	0.416	0.635	1.81
		(ii) 0.5 p.u to 1 p.u load torque from 2 to 5 s for the reference speed 0.5 p.u.	0.192	0.347	0.457	2.12
		(iii) 1 p.u load torque from 5 to 6 s for the reference speed 0.5 p.u.	–	–	–	–
6.0–10.0	157	1 p.u to 0.2 p.u load torque from 6 to 10 s for the reference speed 1 p.u.	0.319	0.508	0.958	Not settled
10.0–11.0	94.2	0.2 p.u load torque from 10 to 11 s for the reference speed 0.6 p.u.	0.335	0.498	0.657	Not settled

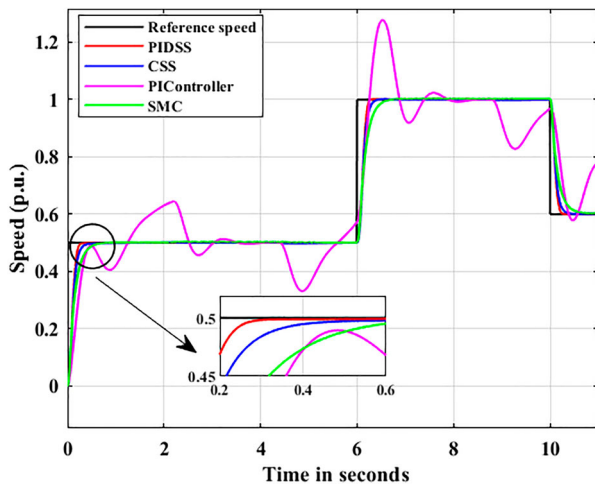


**Figure 28.** Speed response comparison between PI controller, SMC, CSS and PIDSS for undefined load torque-2.

it is decided to implement the servo and regulatory operations of PMDC motor with constant load torque conditions only. The laboratory setup is shown in Figure 29. The setup consists of DC supply, PMDC motor, converter circuit, FPGA controller and 100 MHz digital storage oscilloscope. The permanent magnet DC motor is manufactured by PRANSHU Electricals Pvt. Ltd, Aurangabad, India.

The control algorithms are programmed and uploaded in Spartan-6 XC6SCX9 using Xilinx. After the completion of uploading, the gate pulse is generated to trigger the Insulated Gate Bipolar transistor (FGA25N120).

The specification of sensors used in hardware is given in Table 7.

**Table 6.** Comparison of PI, SMC, CSS and PIDSS for undefined load torque-2.

Time in seconds	Reference speed in rad/sec	Reference speed in per unit	Speed settling time in seconds			
			Third order			
			PIDSS	CSS	SMC	PI
0.0–6.0	78.5	0.5	0.311	0.564	0.758	Not settled
6.0–10.0	157	1	0.317	0.538	0.756	Not settled
10.0–11.0	94.2	0.6	0.268	0.426	0.565	Not settled

**Table 7.** Specifications of sensors.

Sensor type	Model number
Current sensor	HE055T01
Voltage sensor	7840 – Voltage sensing IC
Speed sensor	HEDS5645

The motor is experimentally tested for the initial speed of 750 rpm (0.5 p.u.), then the speed climbs up to the rated rpm and drops to 900 rpm (0.6 p.u.) for constant load torque conditions. The hardware results for PI controller, SMC, CSS, and PIDSS are shown in the figures from Figures 30–43 respectively. The feedback variables used for closed loop operation using PIDSS are more than CSS, SMC and PI controller. Further, computations are higher in PIDSS in comparison with CSS. So, the number of logic cells is incremented in the implementation of PIDSS in FPGA.

Figure 30 shows the changes in armature current, Figure 31 shows the changes armature voltage and Figure 32 shows the combined results of speed, current and voltage for PI controller. Figures 33–35 shows the real time implementation results for SMC. Figure 33

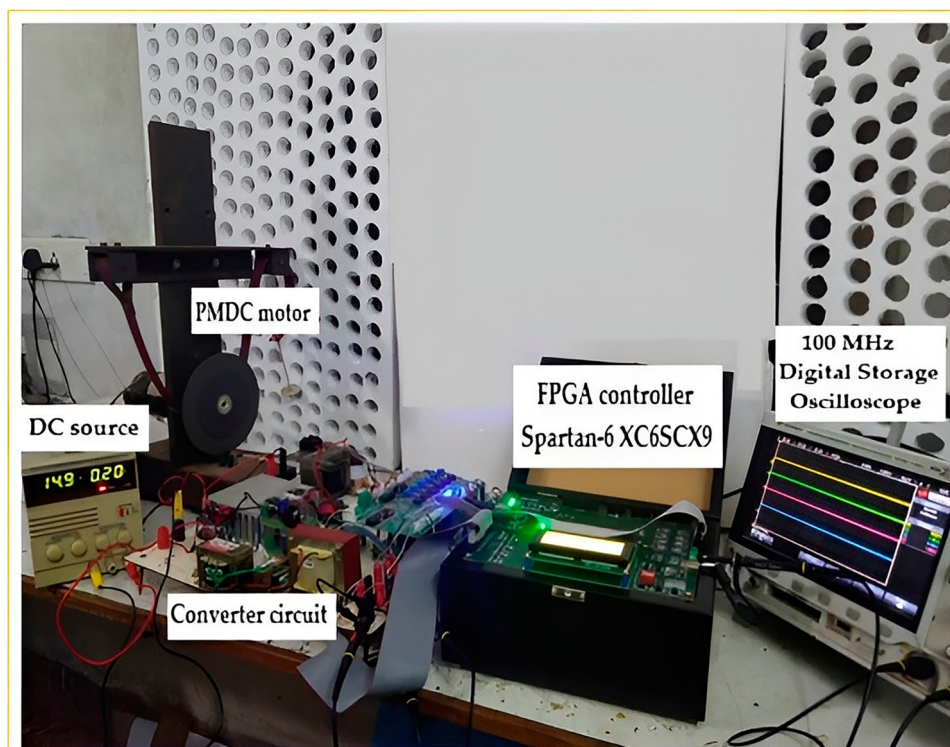


**Figure 29.** Laboratory setup for buck converter fed PMDC motor.

shows the changes in armature current, Figure 34 shows the changes armature voltage and Figure 35 shows the combined results of speed, current and voltage. The results show that no peak overshoot occurs in the implementation of SMC, but the speed tracking is poor in comparison with reference speed profile. In SMC, chattering occurs in the speed tracking.

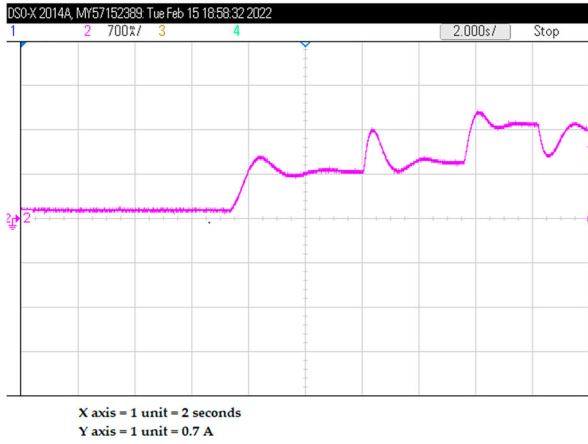


Figure 30. Armature current evolutions for PI controller.

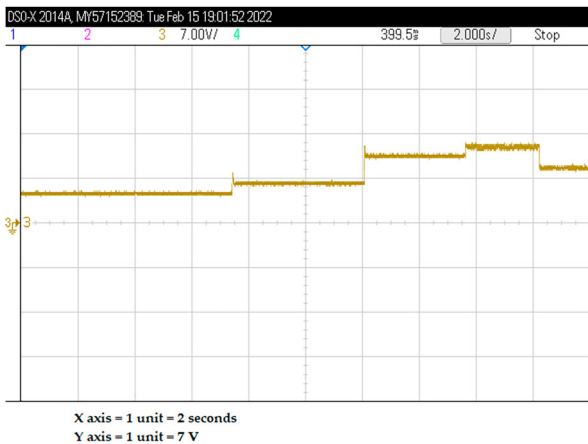


Figure 31. Armature voltage evolutions for PI controller.

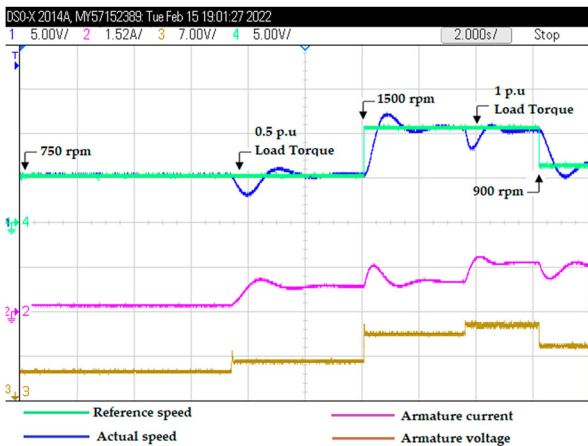


Figure 32. Speed, armature current and armature voltage evolutions for PI controller.

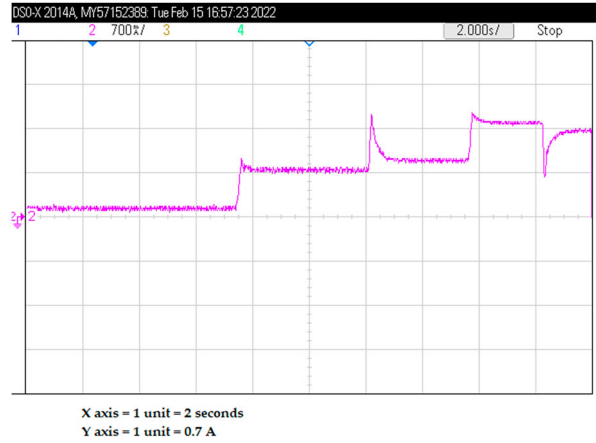


Figure 33. Armature current evolutions for SMC.

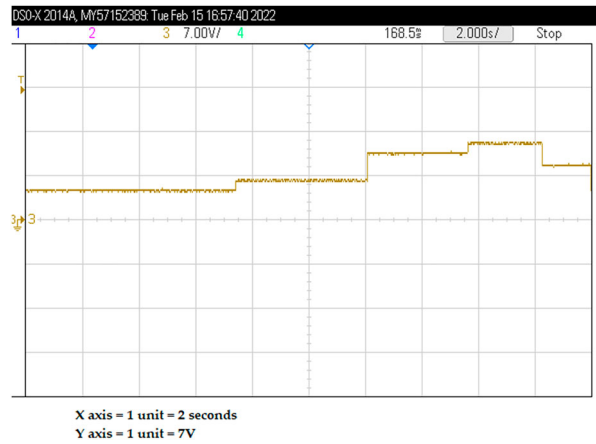


Figure 34. Armature voltage evolutions for SMC.

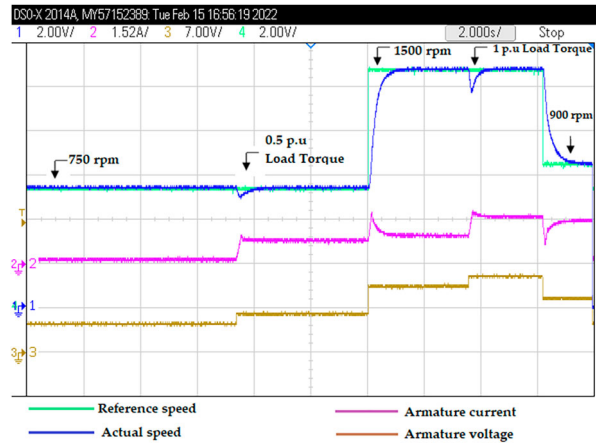


Figure 35. Speed, armature current and armature voltage evolutions for SMC.

Figure 36–38 shows the changes in speed with the reference speed profile, armature voltage and armature current of CSS. Figure 39 displays the combined real time results of speed, armature current and armature voltage of CSS. From the results, no peak overshoot occurs in the implementation of CSS and the settling time is good in comparison with PI and SMC.

Figure 40 depicts the speed evolutions for PIDSS, Figure 41 depicts the armature voltage evolutions for

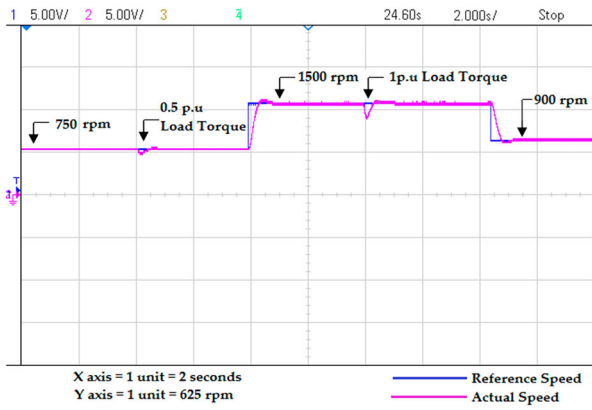


Figure 36. Speed evolutions for CSS.

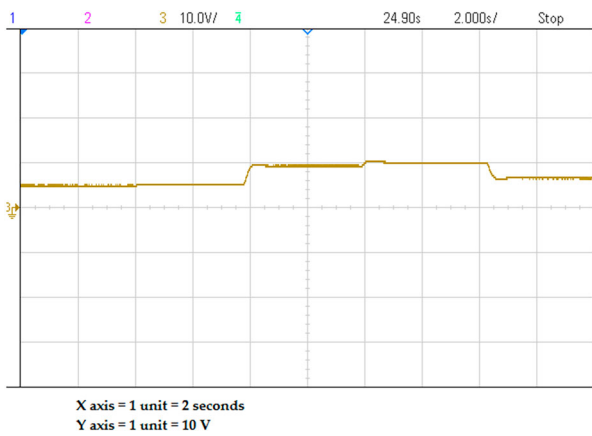


Figure 37. Armature voltage evolutions for CSS.

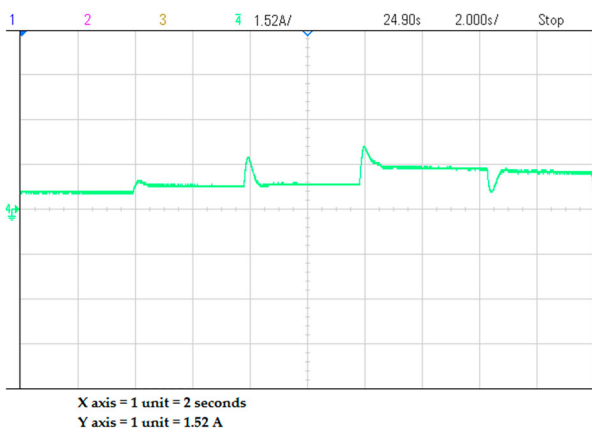


Figure 38. Armature current evolutions for CSS.

PIDSS, Figure 42 depicts the armature current evolutions for PIDSS and Figure 43 depicts the combination of speed, armature voltage, armature current evolutions for PIDSS.

The performance of PI controller, SMC, CSS and PIDSS is evaluated experimentally for constant load torque conditions. In the hardware setup, the settling time of PMDC motor was delayed due to the switching of devices and response of feedback sensors when compared with simulation study. The settling time for PI controller, SMC, CSS and PIDSS in experimental setup for constant load torque is given in Table 8. From the

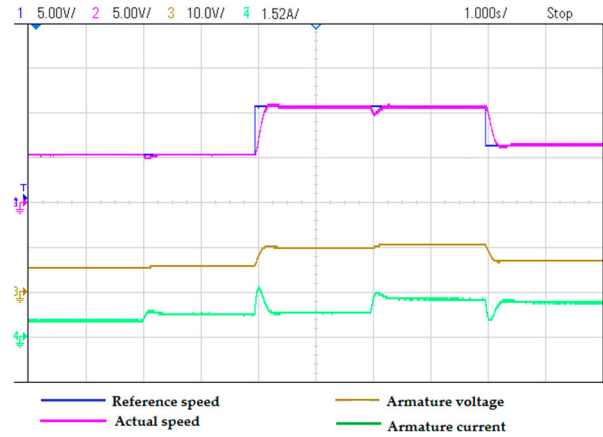


Figure 39. Speed, armature voltage and armature current evolutions for CSS.

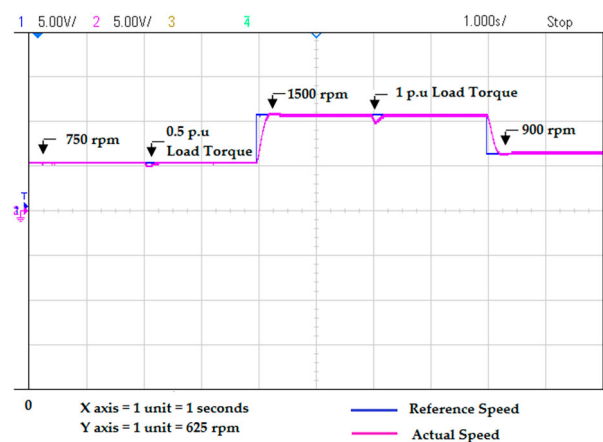


Figure 40. Speed evolutions for PIDSS.

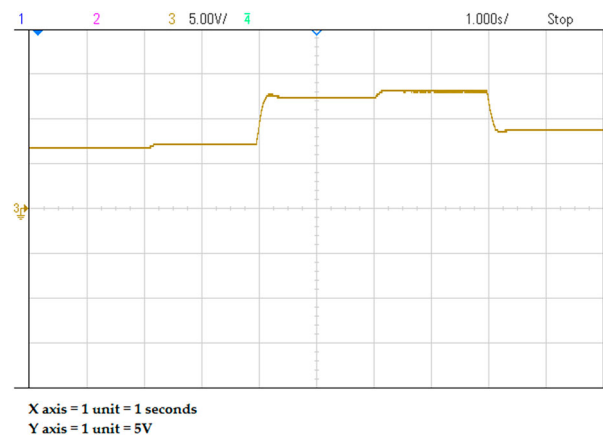
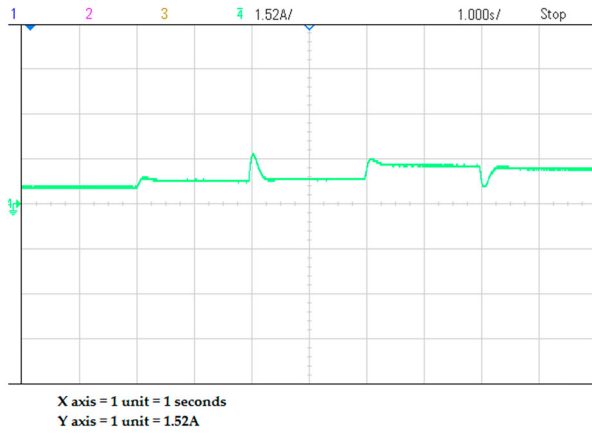


Figure 41. Armature voltage evolutions for PIDSS.

Table 8, the settling time of PIDSS is good during load torque variations with less in chattering and no peak overshoot.

## 8. Conclusion

In this paper third order Proportional Integral Derivative Sliding Surface (PIDSS) third order Classical Siding



**Figure 42.** Armature current evolutions for PIDSS.

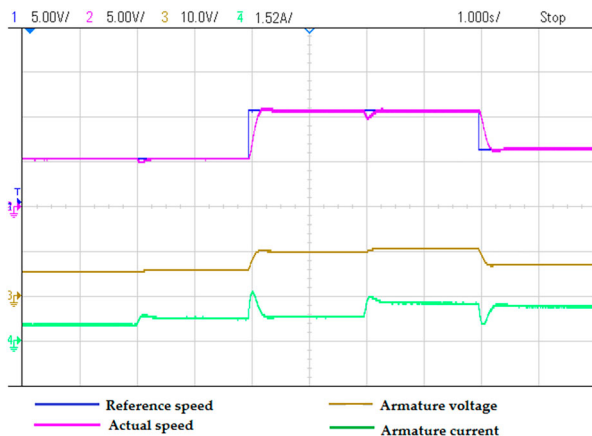


**Figure 43.** Speed, armature voltage and armature current evolutions for PIDSS.

**Table 8.** Comparison of PI, SMC, CSS and PIDSS in experimental setup for constant load torque condition.

Reference speed in rad/sec	Reference speed in per unit	Load torque $T_L$ (p.u.)	Speed settling time in seconds			
			PIDSS	CSS	SMC	PI
78.5	0.5	0.5 p.u	0.25	0.49	0.635	2.05
157	1	0.5 p.u	0.35	0.65	1.15	2.15
157	1	1 p.u	0.3	0.6	0.828	–
94.2	0.6	1 p.u	0.25	0.55	1.05	–

Surface (CSS), Sliding Mode Control (SMC) and Proportional Integral (PI) control algorithms are designed and implemented for buck converter fed PMDC motor. All the algorithms are tested on buck converter fed PMDC motor for no-load condition, constant load torque, frictional load torque, fan type load torque, propeller type load torque and undefined load torque through MATLAB simulation. The robustness of the method is tested with various speeds of PMDC motor. From the simulation results, it is clearly noticed that for load torque variations, the performance of classical sliding surface, SMC and PI control is not satisfactory in settling the speed, chattering elimination and speed tracking in comparison with PIDSS. The PID sliding surface with higher order converges to zero in less time with minimal Integral Square Error. The hardware

results were taken for constant load torque which shows the effectiveness of the proposed control algorithm to regulate the speed of PMDC motor.

Furthermore, the research work can be extended to include the real time implementation of various load torques such as frictional load torque, fan type load torque, propeller type load torque and undefined load torque for higher power ratings of DC motor to enhance the engineering applications. In addition to this four-quadrant operation can be implemented using PIDSS.

## Disclosure statement

No potential conflict of interest was reported by the author(s).

## Funding

The authors thank the Department of Electrical and Electronics Engineering, Anna University, India for the financial support through Rashtriya Uchcharat Shiksha Abhiyan (RUSA) 2.0 (PO 2), Procs. No. 6138/RUSA 2.0/PD3/2018/PO2-1 project.

## ORCID

Dhanasekar Ravikumar  <http://orcid.org/0000-0002-3346-1706>

Ganesh Kumar Srinivasan  <http://orcid.org/0000-0002-4098-6981>

## References

- [1] Shen L. Magnetic functional integrated DC motor drive. *IEEE Access*. 2020;8:5031–5038. DOI:10.1109/ACCESS.2019.2962192.
- [2] Masoud AA, Abu-Ali M, Al-Shaikhi A. Experimental determination of an extended DC servo-motor state space model: an undergraduate experiment. *IEEE Access*. 2020;8:4908–4923. DOI:10.1109/ACCESS.2019.2962612.
- [3] Karnavas YL. Application of recent nature-inspired meta-heuristic optimisation techniques to small permanent magnet DC motor parameters identification problem. *J Eng*. 2020;10:877–888.
- [4] Yoshida N, Takahashi R, Hikihara T. Power regeneration from DC motor with bidirectional router in power packet dispatching system. *IEEE Trans Circuits Syst Express Briefs*. Dec. 2020;67(12):3088–3092.
- [5] Shao Y, Li J. Modeling and switching tracking control for a class of cart-pendulum systems driven by DC motor. *IEEE Access*. 2020;8:44858–44866.
- [6] Jang G, Seo S, Kim C, et al. Self-aligning limited-angle rotary torque PM motor for control valve: design and experimental verification. *IEEE Trans Appl Supercond*. 2020;30:1–5.
- [7] Lopez-Gomez J. Influence of PWM torque control frequency in DC motors by means of an optimum design method. *IEEE Access*. 2020;8:80691–80706.
- [8] Hsu C-H, Huang Y-M. Performance of the noise and vibration of the AC/DC signal for a permanent magnetic DC motor. *IEEE Trans Magn*. 2021;57(2):1–5.
- [9] Sankardoss V, Geethanjali P. PMDC motor parameter estimation using bio-inspired optimization algorithms. *IEEE Access*. 2017;5:11244–11254.

- [10] Soliman WG, Priya BK, Reddy DA, et al. Reconfigurable microarchitecture-based PMDC prototype development for IoT edge computing utilization. *IEEE Sensors J.* 2021;21(2):2334–2345.
- [11] Hoßfeld A, Hiester F, Konigorski U. Analysis of DC motor current waveforms affecting the accuracy of sensorless angle measurement. *IEEE Trans Instrum Meas.* 2021;70:1–8.
- [12] Decarlo RA, Zak SH, Matthews GP. Variable structure control of nonlinear multivariable systems: a tutorial. *Proc IEEE.* 1988;76(3):212–232.
- [13] Hung JY, Gao WB, Hung JC. Variable structure control: a survey. *IEEE Trans Ind Electron.* 1993;40(1):1–22.
- [14] Torelli F, Montegiglio P, Piccinni G, et al. SMC-inspired control approach applied to DC-motor drives. 2020 IEEE International Conference on Environment and Electrical Engineering and 2020 IEEE Industrial and Commercial Power Systems Europe (EEEIC / I&CPS Europe); 2020. p. 1–6. DOI:10.1109/EEEIC/ICPSEurope49358.2020.9160764.
- [15] Rauf A, Zafran M, Khan A, et al. Finite-time nonsingular terminal sliding mode control of converter-driven DC motor system subject to unmatched disturbances. *Int Trans Electr Energy Syst.* 2021;31:1–14.
- [16] Roy TK, Pramanik MAH, Faria F, et al. Speed control of a DC-DC buck converter fed DC motor using an adaptive backstepping sliding mode control approach. 2021 31st Australasian Universities Power Engineering Conference (AUPEC); 2021. p. 1–6. DOI:10.1109/AUPEC52110.2021.9597745.
- [17] Wang J, Rong J, Yu L. Reduced-order extended state observer based event-triggered sliding mode control for DC-DC buck converter system with parameter perturbation. *Asian J Contr.* 2021;23:1591–1601. DOI:10.1002/asjc.2301.
- [18] Li J, Wu A. Digital current-limited sliding-mode control for synchronous buck converter with curved switching surface. *Int J Circ Theor Appl.* 2021;49:536–553. DOI:10.1002/cta.2875.
- [19] Rauf A, Li S, Madonski R, et al. Continuous dynamic sliding mode control of converter-fed DC motor system with high order mismatched disturbance compensation. *Trans Inst Meas Contr.* 2020; 42(14):2812–2821.
- [20] Komurcugil H. Sliding mode control strategy with maximized existence region for DC–DC buck converters. *Int Trans Electr Energy Syst.* 2021;31:e12764. DOI:10.1002/2050-7038.12764.
- [21] Belkaid A, Colak I, Kayisli K, et al. Indirect sliding mode voltage control of buck converter. 2020 8th International Conference on Smart Grid (icSmartGrid), Paris, France, 2020. p. 90–95.
- [22] Zheng C, Dragičević T, Zhang J, et al. Composite robust quasi-sliding mode control of DC–DC buck converter with constant power loads. *IEEE J Emerg Sel Top Power Electron.* April 2021;9(2):1455–1464. DOI:10.1109/JESTPE.2020.3021942.
- [23] Cheng Y, Wen G, Du H. Design of robust discretized sliding mode controller: analysis and application to buck converters. *IEEE Trans Ind Electron.* Dec. 2020;67(12):10672–10681. DOI:10.1109/TIE.2019.2962473.
- [24] Wang Z, Li S, Li Q. Discrete-time fast terminal sliding mode control design for DC–DC buck converters with mismatched disturbances. *IEEE Trans Indus Inform.* Feb. 2020;16(2):1204–1213. DOI:10.1109/TII.2019.2937878.
- [25] Merabet A. Cascade second order sliding mode control for permanent magnet synchronous motor drive. *Electronics.* Dec. 2019;8(12):1508. DOI:10.3390/electronics8121508.
- [26] Rauf A, Yang J, Madonski R, et al. Sliding mode control of converter-fed DC motor with mismatched load torque compensation. 2019 IEEE 28th International Symposium on Industrial Electronics (ISIE), Vancouver, BC, Canada; 2019. p. 653–657.
- [27] Heidarpour S, Tabatabaei M, Khodadadi H. Speed control of a DC motor using a fractional order sliding mode controller. 2017 IEEE International Conference on Environment and Electrical Engineering and 2017 IEEE Industrial and Commercial Power Systems Europe (EEEIC / I&CPS Europe); 2017. p. 1–4. DOI:10.1109/EEEIC.2017.7977822.
- [28] Dhanasekar R, Kumar SG, Rivera M. Third order sliding mode control of buck converter fed permanent magnet DC motor. 2018 IEEE International Conference on Automation/XXIII Congress of the Chilean Association of Automatic Control (ICA-ACCA); 2018. p. 1–4.
- [29] Lavanya M, Brisilla RM, Sankaranarayanan V. Higher order sliding mode control of permanent magnet DC motor. 2012 12th International Workshop on Variable Structure Systems, Mumbai, Maharashtra; 2012. p. 226–230.
- [30] Linares-Flores J, Sira-Ramírez H. Sliding mode-delta modulation GPI control of a DC motor through a buck converter. *IFAC Proc.* 2004;37(21):405–410.
- [31] Alattas KA, et al. Nonsingular terminal sliding mode control based on adaptive barrier function for nth-order perturbed nonlinear systems. *Mathematics.* Dec. 2021;10(1):43. DOI:10.3390/math10010043.
- [32] Nasiri M, Mobayen S, Arzani A. PID-type terminal sliding mode control for permanent magnet synchronous generator based enhanced wind energy conversion systems. *CSEE J Power Energy Syst.* 2022;8(4):993–1003. DOI:10.17775/CSEEJPES.2020.06590
- [33] Goel A, Mobayen S. Adaptive nonsingular proportional–integral–derivative-type terminal sliding mode tracker based on rapid reaching law for nonlinear systems. *J Vib Contr.* 2021;27(23–24):2669–2685. DOI:10.1177/1077546320964287.
- [34] Utkin VI, Gulder J, Shi J. Sliding mode control in electromechanical systems. London: Taylor & Francis; 1999.
- [35] Utkin V. Discussion aspects of high-order sliding mode control. *IEEE Trans Autom Contr.* 2016;61(3):829–833.
- [36] Fridman L, Barbot J-P, Plestan F. Recent trends in sliding mode control. *IET Contr Robotics Sens Series;* 2016. p.1–504.
- [37] Levant A. Homogeneity approach to high-order sliding mode design. *Automatica.* 2005;41:823–830.
- [38] Komurcugil H, Biricik S, Bayhan S, et al. Sliding mode control: overview of its applications in power converters. *IEEE Ind Electron Mag.* March 2021;15(1):40–49. DOI:10.1109/MIE.2020.2986165
- [39] Ziegler JG, Nichols NB. Optimum settings for automatic controllers. *ASME J Dyn Sys Meas Contr.* 1993;115(2B):220–222. DOI:10.1115/1.2899060.